

# Synthesis and Characterization of New Intramolecular C–H Activated Rhodium(III) and Iridium(III) Complexes Containing Functionalized Triphenylphosphines

Sven Sjövall, Maria Johansson, and Carlaxel Andersson\*

*Inorganic Chemistry 1, Centre for Chemistry and Chemical Engineering, Lund University, P.O. Box 124, S-221 00 Lund, Sweden*

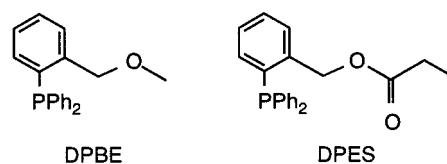
Received November 16, 1998

The hemilabile tertiary phosphine ether and phosphine ester compounds *o*-Ph<sub>2</sub>PC<sub>6</sub>H<sub>4</sub>CH<sub>2</sub>-OMe (DPBE) and *o*-Ph<sub>2</sub>PC<sub>6</sub>H<sub>4</sub>CH<sub>2</sub>OC(O)Et (DPES) and their reactions with different Rh(I) and Ir(I) precursor complexes have been investigated. It is shown that both DPBE and DPES are capable of undergoing oxidative metal insertions at the benzylic positions with the displaced protons appearing as apical hydride ligands in the resulting octahedral complexes. The solution structures of all oxidative addition adducts have been unambiguously identified by various NMR techniques. Also, single-crystal X-ray diffraction studies have been performed for the complexes [RhCl(2,5-NBD)(DPES)] and [IrH(1,5-COD)(DPES)][BF<sub>4</sub>].

## Introduction

Cyclometalated transition-metal complexes are becoming increasingly important in catalysis.<sup>1</sup> Complexes formed by intramolecular insertion of a transition metal into sp<sup>2</sup> C–H bonds have for instance been used in dehydrogenation,<sup>2</sup> coupling,<sup>3</sup> insertion,<sup>4</sup> hydrogenation,<sup>5</sup> addition,<sup>6</sup> activation of hydrocarbons,<sup>7</sup> and asymmetric reactions.<sup>8</sup> Catalytic applications could also be extended to transition-metal complexes with intramolecular metal insertion into sp<sup>3</sup> C–H bonds. However, to the best of our knowledge, there are only a few reports of this being successful. Palladacycles, formed by benzylic C–H activation of tri-*o*-tolylphosphine or 1,3-bis[(diisopropylphosphino)methyl]-2,4,6-trimethylbenzene, are extremely efficient catalysts in the Heck reaction.<sup>9</sup> Therefore, developing new functionalized tertiary phosphines ca-

Chart 1. Structures of the Hemilabile Tertiary Phosphines DPBE and DPES



pable of forming metallacycles by intramolecular metal insertion into sp<sup>3</sup> C–H bonds could be of importance in catalysis.

In this article we report our attempts to elicit insertion of transition-metal centers into tertiary phosphine ligands containing benzylic C–H bonds adjacent to a methoxy or an ester group. By using a functionalized tertiary phosphine (called hemilabile when it possesses a multidentate capacity due to hard and soft donor groups), with an available chelating side chain, cyclometalation can be obtained through chelate-assisted intramolecular oxidative insertion by a transition-metal center. This has been achieved with C–H, N–H, Si–H, O–H, and C–C bonds.<sup>10</sup> The tertiary phenylphosphines used in this article are *o*-Ph<sub>2</sub>PC<sub>6</sub>H<sub>4</sub>CH<sub>2</sub>OMe (DPBE) and *o*-Ph<sub>2</sub>PC<sub>6</sub>H<sub>4</sub>CH<sub>2</sub>OC(O)Et (DPES) (Chart 1). Both DPBE and DPES have oxygen as the heteroatom, directing the benzylic group in the vicinity of the transition-metal center. The donor strengths of the heteroatoms, the steric bulk of the phosphine ligands, the relative stability between different chelate sizes, and the electron densities at the transition-metal centers are expected to govern the preferred coordination modes.

(1) (a) Steenwinkel, P.; Gossage, R. A.; van Koten, G. *Chem. Eur. J.* **1998**, *4*, 759. (b) Ryabov, A. D. *Chem. Rev.* **1990**, *90*, 403.

(2) (a) Gupta, M.; Hagen, C.; Flescher, R. J.; Kaska, W. C.; Jensen, C. M. *Chem. Commun.* **1996**, 2083. (b) Gupta, M.; Kaska, W. C.; Jensen, C. M. *Chem. Commun.* **1997**, 461. (c) Gupta, M.; Kaska, W. C.; Cramer, R.; Jensen, C. M. *J. Am. Chem. Soc.* **1997**, *119*, 840. (d) Xu, W.-W.; Rosini, G. P.; Gupta, M.; Jensen, C. M.; Kaska, W. C.; Krogh-Jespersen, K.; Goldman, A. S. *Chem. Commun.* **1997**, 2273.

(3) (a) van Koten, G. *Pure Appl. Chem.* **1994**, *66*, 1455. (b) Ohff, M.; Ohff, A.; van der Boom, M. E.; Milstein, D. *J. Am. Chem. Soc.* **1997**, *119*, 11687.

(4) (a) Canty, A. J.; van Koten, G. *Acc. Chem. Res.* **1995**, *28*, 406. (b) Donkervoort, J. G.; Vicario, G. L.; Jastrzebski, J. T. B. H.; Gossage, R. A.; Cahiez, G.; van Koten, G. *J. Organomet. Chem.* **1998**, *558*, 61.

(5) (a) Lewis, L. N. *J. Am. Chem. Soc.* **1986**, *108*, 743. (b) Bedford, R. B.; Castillón, S.; Chaloner, P. A.; Claver, C.; Fernandez, E.; Hitchcock, P. B.; Ruiz, A. *Organometallics* **1996**, *15*, 3990. (c) Bianchini, C.; Barbaro, P.; Scapacci, G.; Farnetti, E.; Graziani, M. *Organometallics* **1998**, *17*, 3308.

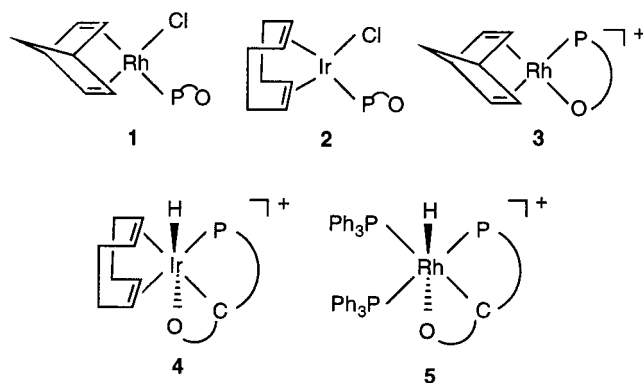
(6) (a) Knapen, J. W. J.; van der Made, A. W.; de Wilde, J. C.; van Leeuwen, P. W. N. M.; Wijkens, P.; Grove, D. M.; van Koten, G. *Nature* **1994**, *372*, 659. (b) Grove, D. M.; van Koten, G.; van Beek, J. A. M. *J. Organomet. Chem.* **1989**, *372*, C1.

(7) (a) Nemah, S.; Jensen, C.; Binamira-Soriaga, E.; Kaska, W. C. *Organometallics* **1983**, *2*, 1442. (b) Rybtchinski, B.; Vignalok, A.; Ben-David, Y.; Milstein, D. *J. Am. Chem. Soc.* **1996**, *118*, 12406.

(8) (a) Gorla, F.; Togni, A.; Venanzi, L. M.; Albinati, A.; Lianza, F. *Organometallics* **1994**, *13*, 1607. (b) Longmire, J.; Xumu, Z. *Organometallics* **1998**, *17*, 4374.

(9) (a) Herrmann, W. A.; Brossmer, C.; Reisinger, C.; Riermeier, T. H.; Öfele, K.; Beller, M. *Chem. Eur. J.* **1997**, *3*, 1357. (b) Beller, M.; Riermeier, T. H. *Eur. J. Inorg. Chem.* **1998**, 29. (c) Reference 3b.

(10) For examples see: (a) Crabtree, R. H. *Chem. Rev.* **1985**, *85*, 245. (b) Hedden, D.; Roundhill, D. M. *Inorg. Chem.* **1986**, *25*, 9. Hedden, D.; Roundhill, D. M.; Fultz, W. C.; Rheingold, A. R. *J. Am. Chem. Soc.* **1984**, *106*, 5014. (c) Auburn, M. J.; Holmes-Smith, R. D.; Stobart, S. R. *J. Am. Chem. Soc.* **1984**, *106*, 1314. (d) Landvatter, E. F.; Rauchfuss, T. B. *Organometallics* **1982**, *1*, 506. (e) Reference 7b.

**Chart 2. Structures of Complexes 1–5 with the Ligand DPES**

### Results and Discussion

In general, intramolecular C–H activation is possible by synthesizing complexes containing metal centers which have at least two vacant coordination sites and which readily undergo oxidative addition. Such complexes are known for all platinum group transition metals, and in the present study we have chosen to work with Rh(I) and Ir(I) complexes.

**Transition-Metal Complexes with DPES.** Treatment of the olefin dimer  $[\mu\text{-MCl}(\text{diene})_2]$  with 2 equiv of the tertiary phosphine *o*-(diphenylphosphino)benzoic acid ethyl ester (DPES) results in the expected bridge cleavage, forming the complexes  $[\text{MCl}(\text{diene})(\text{DPES})]$  from their respective reactions ( $\text{M} = \text{Rh}, \text{Ir}$ ; diene = 2,5-NBD, 1,5-COD). Both **1** and **2** are 4-coordinate with the monodentately coordinated P atom donor cis to the chloride atom (Chart 2). The spectroscopic properties of **1** and **2** are similar (Table 1). Both complexes exhibit  $^{31}\text{P}$  NMR signals shifted about 30–40 ppm downfield from those of uncoordinated DPES, and the value of  $^1J_{\text{RHP}}$  for **1** is typical for a rhodium(I)-complexed monodentate phosphine ligand trans to an olefin.<sup>11</sup> Also, the IR spectroscopic analysis reveals the ester carbonyl stretching frequency at  $1737\text{ cm}^{-1}$  for both **1** and **2**, which exactly matches the frequency for free DPES. Apparently, intramolecular insertion into the benzylic C–H bond does not occur in these neutral complexes, although analogous transition-metal complexes with *o*- $\text{Ph}_2\text{PC}_6\text{H}_4\text{CHO}$  as the hemilabile ligand have previously been found to undergo intramolecular C–H addition.<sup>12</sup>

The reluctance of **1** and **2** to undergo C–H oxidative addition may be due to the absence of any intramolecular interaction between the hinged functional group and the metal center.<sup>10b</sup> By removal of the Cl atom from **1** and **2**, with a halide-abstracting agent, an intramolecular chelate formed by bidentate coordination of the hemilabile DPES ligand is expected, bringing the benzylic group in the vicinity of the transition-metal center. An alternative way to form such cationic 4-coordinate  $d^8$  complexes is the reaction of DPES with the complex  $[\text{M}(\text{diene})_2][\text{X}]$ . We have chosen this latter method and

reacted  $[\text{M}(\text{diene})_2][\text{X}]$  with 1 equiv of DPES to prepare  $[\text{Rh}(2,5\text{-NBD})(\text{DPES})][\text{CF}_3\text{SO}_3]$  (**3**) and  $[\text{Ir}(1,5\text{-COD})(\text{DPES})][\text{BF}_4]$  (**4**) from their respective reactions (Chart 2).

For complex **3**, the IR spectrum clearly demonstrates that the ester carbonyl oxygen is coordinated to the rhodium center, thus forming an eight-membered P,O-chelating ligand (Table 1). Also, the  $^{31}\text{P}\{^1\text{H}\}$  NMR spectroscopic analysis is consistent with a 4-coordinate Rh(I) monomer (Table 1). To be able to detect all olefinic resonances in the 2,5-NBD ligand, the  $^1\text{H}$  NMR spectroscopic investigation of **3** was performed at  $-40\text{ }^\circ\text{C}$ . The loss of information in the room-temperature spectrum probably results from weak coordination of the ester group, which allows a dynamic behavior, although an isomerization process of the square-planar complex cannot be ruled out. It is worth noting that the  $^{31}\text{P}\{^1\text{H}\}$  NMR chemical shift for **3** shows a very small ring shift effect due to chelation, and the  $^1J_{\text{RHP}}$  value is virtually the same as for **1**. The elemental analysis is somewhat unsatisfactory, and related complexes have been reported to be thermally unstable.<sup>10b</sup>

Complex **4** is an off-white powder like many other octahedral hydrido-iridium(III) derivatives.<sup>13</sup> It is very stable and does not react with an additional 1 equiv of DPES under an atmosphere of molecular hydrogen at ambient conditions. The  $^1\text{H}$  NMR spectrum of **4** exhibits a hydride signal as a doublet at  $-19.2\text{ ppm}$ , and the remaining benzylic proton gives rise to a doublet at  $6.87\text{ ppm}$ . Irradiation of the  $^{31}\text{P}$  signal at  $33.9\text{ ppm}$  results in collapse of both these signals into singlets. The coupling constant  $^2J_{\text{PH}}$  ( $13\text{ Hz}$ ) at  $-19.2\text{ ppm}$  is of normal magnitude,<sup>14</sup> but the  $^3J_{\text{PH}}$  value ( $1.8\text{ Hz}$ ) at  $6.87\text{ ppm}$  is surprisingly low for a cyclometalated species.<sup>15</sup> The methylene protons of the terminal ethyl group resonate as a multiplet, implying the appearance of conformers. We believe restricted rotation of the ester group, due to coordination, is the probable cause for this. IR spectroscopy also provides evidence for the coordination of the ester carbonyl oxygen and the presence of a hydride ligand (Table 1). The rather high Ir–H stretching frequency ( $2210\text{ cm}^{-1}$ ) indicates that the hydride is situated trans to a ligand low in the trans-influence series, i.e., the ester carbonyl.<sup>16</sup> An HMQC NMR experiment gives further verification of a cyclometalated species; the broad  $^{13}\text{C}$  signal at  $92.3\text{ ppm}$  correlates with the  $^1\text{H}$  signal at  $6.87\text{ ppm}$ .

Since the hydride, the alkene  $\pi$ -bond, and the iridium center in **4** are coplanar, the exclusive cis addition of the metal hydride to the alkene would be expected.<sup>17</sup> The reason for the reluctance of this migratory insertion reaction is not obvious. Most probably, extensive polarization of the electron density from the metal center toward the diene creates a particularly strong Ir–H bond. Also, an equilibrium between **4** and a 16-electron Ir(III)  $\eta^1:\eta^2$  adduct in solution could also be possible. However, we rule this out, since the NMR spectroscopic

(11) Pregosin, P. S.; Kunz, R. W.  *$^{31}\text{P}$  and  $^{13}\text{C}$  NMR of Transition Metal Phosphine Complexes*; Springer-Verlag: New York, 1979.

(12) (a) Rauchfuss, T. B. *J. Am. Chem. Soc.* **1979**, *101*(4), 1045. (b) Ko, J.; Joo, W. C. *Bull. Korean Chem. Soc.* **1987**, *8*, 372. (c) Gao, J.-X.; Wang, J.-Z.; Hu, S.-Z.; Wan, H.-L. *Gaodeng Xuexiao Huaxue Xuebao* **1995**, *16*, 666.

(13) Werner, H.; Schulz, M.; Windmüller, B. *Organometallics* **1995**, *14*, 3659.

(14) For examples see ref 7b.

(15) Sjövall, S.; Kloos, L.; Nikitidis, A.; Andersson, C. *Organometallics* **1998**, *17*, 579.

(16) Jesson, J. P. *Transition Metal Hydrides*; Muetterties, E. L., Ed.; Dekker: New York, 1971; Chapter 4.

(17) James, B. R. *Compr. Organomet. Chem.* **1982**, *8*, 306.

**Table 1.**  $^{31}\text{P}\{^1\text{H}\}$  NMR Data (ppm) and IR Spectral Data ( $\text{cm}^{-1}$ )

complex	$^{31}\text{P}$ NMR <sup>a</sup>			IR		complex	$^{31}\text{P}$ NMR <sup>a</sup>			IR <sup>h</sup>	
	$\delta$	$^1J_{\text{RhP}}$	$^2J_{\text{PP}}$	$\nu(\text{C}=\text{O})$	$\nu(\text{M}-\text{H})$		$\delta$	$^1J_{\text{RhP}}$	$^2J_{\text{PP}}$	$\nu(\text{O}-\text{Me})$	$\nu(\text{M}-\text{H})$
DPES <sup>b,f</sup>	-15.8 s			1737 s		DPBE <sup>b,f</sup>	-14.8 s			1065 s	
<b>1</b> <sup>b,f</sup>	24.3 d	166		1737 s		<b>6</b> <sup>b,f</sup>	23.2 d	169		1030 m	
<b>2</b> <sup>b,f</sup>	17.4 s			1737 s		<b>7</b> <sup>c,f</sup>	11.0 s			1031 s	
<b>3</b> <sup>c,f</sup>	21.6 d	165		1711 m		<b>8</b> <sup>b,f</sup>	49.7 d	204		1038 s	
<b>4</b> <sup>b,g</sup>	33.9 s			1593 m	2210 w	<b>9a</b> <sup>d,g</sup>	25.8 d		390	1047 s	2210 w
<b>5</b> <sup>c,g</sup>	54.5 ddd	113	368, 22.4				6.0 d		390	1069 m	
	40.2 ddd	110	368, 24.1	1617 m	2127 w	<b>9b</b> <sup>d,g</sup>	16.2 bs			1047 s	2210 w
	25.3 dt	85.6	22.1				5.3 bs			1069 m	

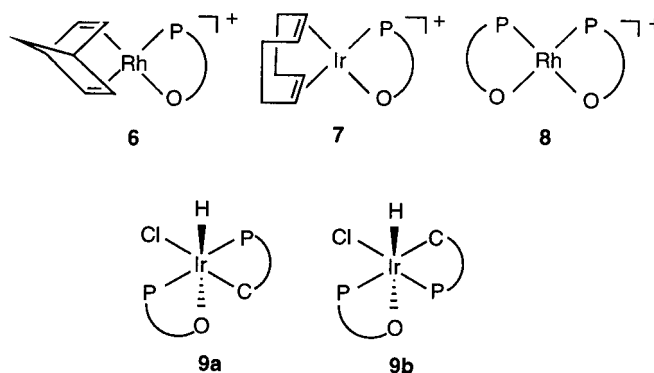
<sup>a</sup> All  $J$  values in Hz. <sup>b</sup>  $^{31}\text{P}\{^1\text{H}\}$  NMR in  $\text{CDCl}_3$ . <sup>c</sup>  $^{31}\text{P}\{^1\text{H}\}$  NMR in  $\text{CD}_2\text{Cl}_2$ . <sup>d</sup>  $^{31}\text{P}\{^1\text{H}\}$  NMR in  $\text{C}_6\text{D}_6$ . <sup>e</sup>  $^{31}\text{P}\{^1\text{H}\}$  NMR in  $\text{CD}_2\text{Cl}_2$  at  $-40^\circ\text{C}$ . <sup>f</sup> IR spectra obtained in  $\text{CH}_2\text{Cl}_2$ . <sup>g</sup> KBr disk. <sup>h</sup> The assignments of the  $\nu(\text{O}-\text{Me})$  bands are tentative because of the possibilities of overlapping stretching frequencies.

analyses did not reveal any isomerization of the coordinated diene.

So far we have not effected intramolecular insertion of a rhodium center into the benzylic C–H bond of the DPES ligand. Apparently, as seen for complex **3**, bidentate coordination of the hemilabile DPES ligand alone is insufficient to elicit the oxidative-addition reaction. It could well be that the  $\pi$ -accepting diene ligand decreases the electron density at the rhodium center to such an extent that C–H activation is rendered impossible.<sup>10b,15</sup> If the diene ligand in **3** were replaced with  $\sigma$ -donating phosphine ligands, a significantly larger electron density would be imparted on the transition-metal center, and this could be a fruitful way to achieve the desired oxidative-addition reaction. We have therefore replaced the 2,5-NBD ligand with such stronger electron donors.

Complex **5** was synthesized by treating the precursor  $[\text{Rh}(\text{PPh}_3)_2(2,5\text{-NBD})][\text{PF}_6]$  with 1 equiv of DPES under an atmosphere of molecular hydrogen. The IR spectrum suggests that the carbonyl oxygen of the DPES ligand is coordinated to the rhodium center and also reveals a Rh–H band at  $2127\text{ cm}^{-1}$  (Table 1), which is characteristic of a hydride ligand on Rh(III) trans to a ligand low in the trans-influence series.<sup>16</sup> Analysis of the  $^{31}\text{P}\{^1\text{H}\}$  NMR spectrum, performed at  $-40^\circ\text{C}$  to decrease line width, exhibits three different signals; ABCX patterns occur at 54.5 and 40.2 ppm, and an  $\text{A}_2\text{BX}$  pattern appears at 25.3 ppm (Table 1). The two downfield signals indicate two  $^2J_{\text{PP}}$  couplings each, both normal for phosphorus atoms situated trans or cis to each other, respectively. The low-field resonance at 54.5 ppm is assigned to the cyclometalated DPES ligand.<sup>15</sup> The upfield resonance at 25.3 ppm displays a somewhat broad doublet of triplets resulting from two cis  $^2J_{\text{PP}}$  coupling constants of virtually the same magnitude. Finally, the small  $^1J_{\text{RhP}}$  coupling constant (85.6 Hz) apparent from the signal at 25.3 ppm implies that this  $\text{PPh}_3$  ligand is coordinated trans to a highly trans-influencing atom, i.e., the metallacyclic benzylic carbon. These data are only compatible with the chemical composition  $[\text{Rh}(\text{PPh}_3)_2(\text{DPES})][\text{PF}_6]$ , and the only possible coordination geometry for complex **5** is depicted in Chart 2.

Further verification of the proposed structure of **5** is provided by its  $^1\text{H}$  NMR spectrum, which exhibits two characteristic signals with an intensity equal to one hydrogen each: a doublet of doublet of triplets at  $-17.3$  ppm and a broad doublet at 6.09 ppm. By performing  $^1\text{H}\{^{31}\text{P}\}$  NMR spectroscopy, we can determine the coupling constants:  $^1J_{\text{RhH}} = 20$  Hz,  $^2J_{\text{PH}} = 16, 10$  Hz at

**Chart 3.** Structures of Complexes **6–9** with the Ligand DPBE

$-17.4$  ppm and  $^2J_{\text{RhH}} = 20$  Hz at 6.09 ppm. The magnitudes of the  $^2J_{\text{PH}}$  coupling constants are consistent with all phosphorus atoms being cis to the hydride. Final confirmation of metallacyclic formation in **5** is given by its  $^{13}\text{C}\{^1\text{H}\}$  and HMQC NMR spectroscopic data; the benzylic  $^{13}\text{C}$  resonance appears at 103.8 ppm ( $^1J_{\text{RhC}} = 87$  Hz,  $^2J_{\text{PC}} = 23, 10, 3$  Hz), and it correlates with the benzylic  $^1\text{H}$  resonance at 6.09 ppm.

**Transition-Metal Complexes with DPBE.** As shown, oxidative insertion of a rhodium or iridium center into the benzylic C–H bond of DPES is facile, given the correct conditions. Use of these same strategies with  $\sigma$ -(diphenylphosphino)benzoic acid methyl ether (DPBE) as the ligand have also been investigated.

The complexes  $[\text{Rh}(2,5\text{-NBD})(\text{DPBE})][\text{CF}_3\text{SO}_3]$  (**6**) and  $[\text{Ir}(1,5\text{-COD})(\text{DPBE})][\text{BF}_4]$  (**7**) were synthesized by methods analogous to that of **3** (Chart 3). The IR spectroscopic measurements reveal the stretching frequencies for the OMe bands at 1030 (**6**) and  $1031\text{ cm}^{-1}$  (**7**), respectively (Table 1). These shifts of the ether vibrations to lower wavenumbers, compared to that of free DPBE ( $1065\text{ cm}^{-1}$ ), are explicable in terms of ring closure of the DPBE ligand.<sup>18</sup> The existence of six-membered P,O-chelates is further substantiated by the NMR spectroscopic investigations. In the  $^1\text{H}$  NMR spectra of **6** and **7**, the methyl resonances are shifted 0.3–0.5 ppm downfield of that observed for free DPBE due to coordination of the ether oxygen, which results in deshielding of the adjacent hydrogens.<sup>19</sup> The  $^{31}\text{P}\{^1\text{H}\}$  NMR spectrum of **6** resembles the  $^{31}\text{P}\{^1\text{H}\}$  NMR spectra of **1** and **3** (Table 1).

(18) Bader, A.; Lindner, E. *Coord. Chem. Rev.* **1991**, *108*, 27.

(19) Rauchfuss, T. B.; Patino, F. T.; Roundhill, D. M. *Inorg. Chem.* **1975**, *14*, 652.



To impart a greater electron density on the rhodium center, we first carried out a procedure analogous to that employed in the synthesis of **5**, but with DPBE as the hemilabile phosphine ligand. However, there was a tendency for the reaction to lead to a mixture of products. Therefore, the precursor  $[\text{Rh}(2,5\text{-NBD})_2][\text{CF}_3\text{-SO}_3]$  was used instead and treated with 2 equiv of DPBE in the synthesis of the complex  $[\text{Rh}(\text{DPBE})_2][\text{CF}_3\text{SO}_3]$  (**8**) (Chart 3). To enable replacement of both dienes in the precursor, the synthesis of **8** has to be carried out under an atmosphere of molecular hydrogen, which is not the case with tertiary hemilabile alkylphosphines.<sup>19</sup> Oxidative addition of the rhodium center into the benzylic C–H bond does not occur in this complex, although the analogous complex with *o*- $\text{Ph}_2\text{PC}_6\text{H}_4\text{CH}_2\text{N}(\text{CH}_3)\text{C}(\text{O})\text{Et}$  as the hemilabile ligand has previously been found to undergo intramolecular benzylic C–H activation.<sup>15</sup>

The NMR spectroscopic analysis of **8** is consistent with a square-planar Rh(I) complex of cis configuration (Table 1). The  $^{31}\text{P}\{^1\text{H}\}$  NMR spectrum exhibits an  $\text{A}_2\text{X}$  system, with a doublet at 49.7 ppm, caused by two chemically equivalent P atoms. The relatively large  $^1J_{\text{RhP}}$  value is in accordance with the lower trans-influencing ether oxygen atoms being trans to the phosphines.<sup>20</sup> The  $^1\text{H}$  NMR spectrum of **8** is not significantly different from those of the aforementioned complexes **6** and **7**; i.e., the chemical shift for the ether functional groups is consistent with two complexed oxygens. In addition, the IR spectrum also supports the NMR spectra with the stretching frequency for the OMe band at  $1038\text{ cm}^{-1}$  (Table 1). However, the elemental analysis deviated from that calculated with respect to the carbon content, most likely because of a great propensity for the complexes  $[\text{Rh}(\text{P},\text{O})_2]^+$  to decompose.<sup>21</sup>

Clearly, oxidative metal insertion into the DPBE ligand is not as facile as for the DPES ligand. Also, on the basis of the synthesis of complexes **2**, **4**, and **5**, a transition-metal center (i) being from the third transition series, (ii) bearing a higher electron density, and (iii) coordinating the ligand's heteroatom is the most plausible candidate to oxidatively insert into a C–H bond. To fulfill all three criteria and circumvent the need of an atmosphere of hydrogen during the synthesis (cf. complex **8**), we treated the cyclooctene complex  $[\mu\text{-IrCl}(\text{C}_8\text{H}_{14})_2]_2$  with 4 equiv of DPBE to form complex **9**.

From repetition of the synthesis of **9** several times, it is clear that the complex exists as two geometrical isomers in an approximately 1:1 ratio, which we have been unable to separate. However, since the relative isomer yield varies slightly between preparations, we are able to assign those NMR resonances due to **9a** separately from those due to **9b**. The  $^1\text{H}$  NMR spectrum exhibits two hydride signals; a doublet of doublets at  $-19.8\text{ ppm}$  ( $^2J_{\text{PH}} = 21, 11\text{ Hz}$ ) for **9a** and a triplet at  $-20.0\text{ ppm}$  ( $^2J_{\text{PH}} = 16\text{ Hz}$ ) for **9b**. The magnitudes of the coupling constants for both isomers are in accordance with the phosphorus atoms being cis to the hydride. Also, the benzylic protons in the P,O-chelating DPBE ligand appear as coupled doublets and hence are

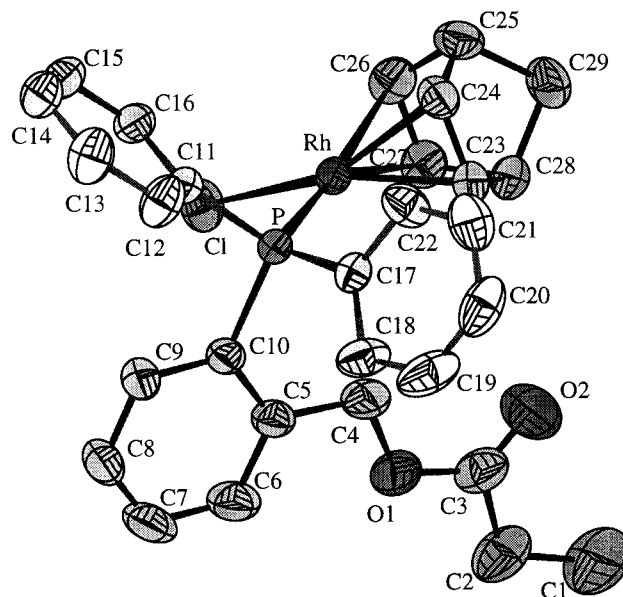


Figure 1. DIAMOND drawing of complex **1**.<sup>22</sup>

diastereotopic. This phenomenon, which lowers the symmetry of the complex, has been detected before in cyclometalated adducts.<sup>15</sup> In the  $^{31}\text{P}\{^1\text{H}\}$  NMR spectrum, **9a** exhibits an ABX pattern with  $^2J_{\text{PP}} = 390\text{ Hz}$ , implying a trans disposition of the P atoms (Table 1). However, we could not detect any coupling for **9b**, since its  $^{31}\text{P}$  signals appeared just as broad singlets. Most likely this is because we have a very small cis  $^2J_{\text{PP}}$  coupling; i.e., the P atoms are trans to highly trans-influencing atoms. For both isomers, the low-field  $^{31}\text{P}$  signal is assigned to the metallated DPBE ligand.<sup>15</sup> The IR spectrum of **9** shows the presence of a hydride and both coordinated and uncoordinated ether groups (Table 1). The broad band at  $2210\text{ cm}^{-1}$  can be taken as indicative of a hydride ligand on Ir(III) trans to a ligand low in the trans-influence series.<sup>16</sup> Also, the coordinated OMe group, which gives rise to an absorption at  $1047\text{ cm}^{-1}$ , shows only a weak ring shift. These IR properties are only explicable if the hydride ligand and the coordinated ether group are situated trans to each other. Hence, the spectroscopic data are only compatible with the chemical composition  $[\text{IrHCl}(\text{DPBE})_2]$ , and the geometric isomers are depicted in Chart 3.

Since we could not detect the remaining benzylic protons on the metallacyclic carbons of **9**, it was vital to perform further NMR investigations. In the  $^{13}\text{C}\{^1\text{H}\}$  NMR spectrum two characteristic signals appeared, a doublet at  $91.4\text{ ppm}$  ( $^2J_{\text{PC}} = 98\text{ Hz}$ ) and a broad singlet at  $58.6\text{ ppm}$ . An HMQC NMR experiment verified that these  $^{13}\text{C}$  signals correlate with one doublet each in the  $^1\text{H}$  NMR spectrum, coincidentally lying in the aromatic region.

In summary, from this study it is clear that the hemilabile phosphines DPES and DPBE are capable of oxidatively adding a benzylic C–H bond to a platinum-group metal, given the correct conditions.

**Crystal Structures.** Single crystals of **1** were well-formed yellow plates belonging to the space group  $P\bar{1}$ . A view of the molecular structure is shown in Figure 1, and selected bond distances and angles are listed in Table 2.

(20) Lindner, E.; Wang, Q.; Hermann, A. M.; Fawzi, R.; Steimann, M. *Organometallics* **1993**, *12*, 1865.

(21) Lindner, E.; Andres, B. *Chem. Ber.* **1987**, *120*, 761.

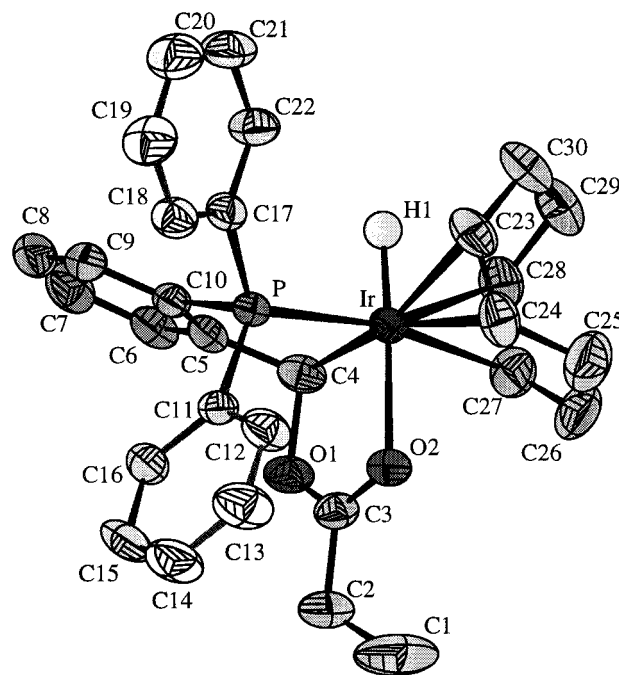
**Table 2. Selected Bond Angles and Distances with Esd's for Complex 1**

Bond Distances (Å)			
Rh–P	2.3016(8)	C3–O1	1.342(4)
Rh–Cl	2.354(1)	C3–O2	1.177(5)
Rh–C23	2.102(3)	C4–O1	1.432(3)
Rh–C24	2.106(3)	C23–C24	1.392(4)
Rh–C26	2.209(3)	C26–C27	1.369(4)
Rh–C27	2.192(3)		
Bond Angles (deg)			
P–Rh–Cl	91.15(4)	Cl–Rh–C24	156.52(9)
P–Rh–C23	98.68(8)	Cl–Rh–C26	96.36(10)
P–Rh–C24	103.57(8)	Cl–Rh–C27	96.32(9)
P–Rh–C26	166.23(9)	Rh–P–C10	112.1(1)
P–Rh–C27	154.05(9)	Rh–P–C11	114.6(1)
Cl–Rh–C23	157.18(8)	Rh–P–C17	116.9(1)

The coordination geometry around the rhodium center is pseudo square planar, illustrated for instance by the bond angle for P–Rh–Cl (91.15(4)°). The greatest deviation from the least-squares plane through the Rh, Cl, and P atoms and the midpoints of the two coordinated carbon double bonds is 0.075 Å for the center between C26 and C27. Due to ring strain in the  $\eta^2:\eta^2$ -coordinating 2,5-NBD ligand, the angle between the central atom and the midpoints of the C23–C24 and C26–C27 double bonds is decreased to 71.8°. The Rh–P (2.3016(8) Å) and Rh–Cl (2.354(1) Å) bond lengths are in good agreement with those reported for the related complex [RhCl(1,5-COD){Ph<sub>2</sub>PNHP(O)Ph<sub>2</sub>-P}],<sup>23</sup> The greater trans influence exerted by the P atom than the Cl atom results in a significant difference in the rhodium to carbon distances of the coordinated diene. Whereas the C23 and C24 atoms (trans to Cl) are located at a distance of 2.102(3) and 2.106(3) Å from the metal center, the Rh–C bond lengths for C26 and C27 (trans to P) are longer by ca. 0.1 Å. In accordance with this, the double-bond length for C26–C27 (1.369(4) Å) is shorter than for C23–C24 (1.392(4) Å). All other bond distances and angles lie in the expected range.

The strong spectroscopic evidence suggesting **4** to be the result of an oxidative addition of a C–H bond to the iridium center has been confirmed by a single-crystal X-ray diffraction investigation. Slow diffusion of diethyl ether into an acetone solution led to the deposition of **4** as colorless plates. Selected bond distances and angles are listed in Table 3.

As seen in Figure 2, the octahedral geometry around the iridium atom is considerably distorted, as illustrated by the bond angles O2–Ir–H1 (171.0(16)°) and C4–Ir–H1 (92.2(16)°). The bond angles P–Ir–C4 and C4–Ir–O2 are decreased to 80.99(14) and 79.4(2) Å, respectively, due to ring strain in the two five-membered chelates. The observed bond distance between the iridium and the hydride atom (1.516(45) Å) is similar to those established for other hydrido-iridium(III) complexes.<sup>24</sup> Also, the Ir–C4 bond length of 2.070(5) Å is in the region of other reported cyclometalated transition-metal complexes.<sup>25</sup> The bond distance for Ir–O2

**Figure 2.** DIAMOND drawing of complex **4**.<sup>22</sup>**Table 3. Selected Bond Angles and Distances with Esd's for Complex 4**

Bond Distances (Å)			
Ir–P	2.290(1)	Ir–C28	2.283(5)
Ir–C4	2.070(5)	Ir–H1	1.516(45)
Ir–O2	2.163(4)	C3–O2	1.262(6)
Ir–C23	2.286(5)	C3–O1	1.277(7)
Ir–C24	2.298(5)	C23–C24	1.372(8)
Ir–C27	2.267(6)	C27–C28	1.374(8)
Bond Angles (deg)			
P–Ir–C4	80.99(14)	C4–Ir–C24	161.1(2)
P–Ir–O2	90.24(10)	C4–Ir–C27	91.5(2)
P–Ir–H1	91.8(15)	C4–Ir–C28	95.1(2)
P–Ir–C23	97.74(14)	O2–Ir–H1	171.0(16)
P–Ir–C24	106.2(2)	O2–Ir–C23	117.1(2)
P–Ir–C27	167.53(15)	O2–Ir–C24	83.0(2)
P–Ir–C28	154.9(2)	O2–Ir–C27	78.5(2)
C4–Ir–O2	79.4(2)	O2–Ir–C28	113.6(2)
C4–Ir–H1	92.2(16)	Ir–C4–O1	107.5(3)
C4–Ir–C23	163.5(2)		

(2.163(4) Å) is significantly shorter than for [IrHCl{ $\kappa^2$ (C,P)-CH<sub>2</sub>OCH<sub>2</sub>CH<sub>2</sub>P-*i*-Pr<sub>2</sub>}]{ $\kappa^2$ (P,O)-*i*-Pr<sub>2</sub>PCH<sub>2</sub>CH<sub>2</sub>-OMe}] (2.339(4) Å) and [IrCl<sub>2</sub>{ $\kappa^2$ (C,P)-CH<sub>2</sub>N(Me)<sub>2</sub>CH<sub>2</sub>-CH<sub>2</sub>P-*i*-Pr<sub>2</sub>}]{ $\kappa^2$ (P,N)-*i*-Pr<sub>2</sub>PCH<sub>2</sub>CH<sub>2</sub>N(Me)<sub>2</sub>}] [Cl] (2.264(6) Å), which probably reflects a higher donor strength of the ester group compared to an ether or amine group.<sup>13</sup> The following properties reveal a very small difference in trans influence between the P and C4 donor: (i) the Ir–C(olefin) distances for Ir–C23 and Ir–C24 are 2.286(5) and 2.298(5) Å, respectively, compared to the values for Ir–C27 (2.267(6) Å) and Ir–C28 (2.283(5) Å); (ii) the respective distances between the sp<sup>2</sup>-carbon atoms in the diene ligand are 1.372(8) Å for C23–C24 and 1.374(8) Å for C27–C28. All other bond distances and angles lie in the expected range.

A comparison of selected structural data of **1** with those of **4** is given in Table 4. From these data it is seen that the side chain in the DPES ligand undergoes few significant structural changes upon cyclometalation; the bond angles for the atoms involved in the metallacycle in **4** are all more acute than in **1**, and the differences in

(22) Brandenburg, K. DIAMOND: Crystal Structure Information System, Version 1.2; 1997.

(23) Slawin, A. M. Z.; Smith, M. B.; Woollins, J. D. *J. Chem. Soc., Dalton Trans.* **1996**, 1283.

(24) Stoutland, P. O.; Bergman, R. G. *J. Am. Chem. Soc.* **1988**, *110*, 5732. Werner, H.; Höhn, A.; Dziallas, M. *Angew. Chem., Int. Ed. Engl.* **1986**, *12*, 1090.

(25) Clark, G. R.; Greene, T. R.; Roper, W. R. *J. Organomet. Chem.* **1985**, *C25*, 293.



**Table 4. Comparison of Structural Data (Bond Lengths in Å, Angles in deg) for Complexes 1 and 4**

	complex 1	complex 4
M <sup>a</sup> –P	2.3016(8)	2.290(1)
P–C10	1.845(3)	1.821(5)
C10–C5	1.402(4)	1.394(6)
C5–C4	1.501(4)	1.502(7)
C4–O1	1.432(3)	1.524(5)
O1–C3	1.342(4)	1.277(7)
C3–O2	1.177(5)	1.262(6)
C3–C2	1.518(5)	1.480(7)
C2–C1	1.476(6)	1.473(15)
M <sup>a</sup> –P–C10	112.79(9)	101.7(2)
P–C10–C5	121.1(2)	112.7(3)
C10–C5–C4	121.5(2)	118.5(4)
C5–C4–O1	109.1(2)	105.9(4)
C4–O1–C3	117.0(3)	117.7(4)
O1–C3–O2	122.8(3)	123.8(5)
O1–C3–C2	109.7(3)	116.5(7)
C3–C2–C1	113.3(4)	116.3(7)

<sup>a</sup>M = Rh (1), Ir (4).

bond distances are all due to coordination of the carbonyl functionality in 4.

### Experimental Section

The apparatuses, general procedures, and purification of solvents have been previously described.<sup>15</sup> Pyridine was dried with powdered potassium hydroxide, followed by distillation over calcium dihydride, and used immediately. Propionyl chloride was distilled and used immediately. Commercially available reagents were purchased and used without further purification. The compound DPBE<sup>19</sup> and the complexes [ $\mu$ -RhCl(2,5-NBD)]<sub>2</sub>,<sup>26</sup> [ $\mu$ -IrCl(1,5-COD)]<sub>2</sub>,<sup>27</sup> [Ir(1,5-COD)]<sub>2</sub>[BF<sub>4</sub>],<sup>28</sup> [Rh(2,5-NBD)]<sub>2</sub>[CF<sub>3</sub>SO<sub>3</sub>],<sup>28</sup> [ $\mu$ -IrCl(C<sub>8</sub>H<sub>14</sub>)<sub>2</sub>],<sup>29</sup> and [Rh(2,5-NBD)-(PPh<sub>3</sub>)<sub>2</sub>][PF<sub>6</sub>]<sup>30</sup> were prepared according to literature procedures. The tertiary phosphines are hygroscopic, but once isolated as pure solids they are relatively stable toward oxygen.

<sup>1</sup>H and <sup>31</sup>P NMR spectra were recorded at 300 and 121 MHz, respectively, using a Varian Unity 300 MHz spectrometer. <sup>13</sup>C and HMQC (2D inverse H,C correlation) NMR spectra were recorded at 125 and 500 MHz, respectively, using a Bruker ARX 500 MHz spectrometer. Unless otherwise stated, the NMR measurements were performed in CDCl<sub>3</sub>.

**Synthesis of  $\sigma$ -(Diphenylphosphino)benzoic Acid Ethyl Ester, ( $\sigma$ -Ph<sub>2</sub>PC<sub>6</sub>H<sub>4</sub>CH<sub>2</sub>OC(O)Et) (DPES).** A solution of  $\sigma$ -(diphenylphosphino)benzyl alcohol<sup>10d</sup> (2.74 g, 9.39 mmol) and pyridine (2.25 g, 28.4 mmol) in THF (10 mL) was vigorously stirred. Propionyl chloride (0.902 g, 9.75 mmol) was added through a septum with a syringe, and the suspension was stirred for 1.5 h. The precipitate was removed by Schlenk filtration and washed with THF (3 × 20 mL). Evaporation of the combined filtrates yielded a yellow, viscous oil. The oil was dissolved in diethyl ether (40 mL), the solution was washed with water (5 × 30 mL), and the organic phase was dried with magnesium sulfate. The solution was filtered and reduced to ca. 2 mL, and *n*-pentane (100 mL) was added to the remaining oil. The cloudy solution was stored overnight at –18 °C, and the resulting white needles were isolated by filtration and dried under vacuum. Yield: 2.0 g (61%). <sup>1</sup>H NMR:  $\delta$  7.48–7.20 (m, 13H, Ar), 6.95 (dd, <sup>3</sup>J<sub>HH</sub> = 7.5, 4.5 Hz, 1H, Ar), 5.35 (bs, 2H, Ar–CH<sub>2</sub>–), 1.95 (q) and 1.94 (q) (<sup>3</sup>J<sub>HH</sub> = 6.6 Hz, 2H,

–CH<sub>2</sub>–), 0.96 (t) and 0.95 (t) (<sup>3</sup>J<sub>HH</sub> = 6.6 Hz, 3H, –CH<sub>3</sub>). Anal. Calcd for C<sub>22</sub>H<sub>21</sub>O<sub>2</sub>P: C, 75.8; H, 6.1; P, 8.9. Found: C, 75.5; H, 6.3; P, 8.9.

**Reaction of [ $\mu$ -RhCl(2,5-NBD)]<sub>2</sub> with DPES. Formation of [RhCl(2,5-NBD)(DPES)] (1).** A dichloromethane solution (10 mL) of [ $\mu$ -RhCl(2,5-NBD)]<sub>2</sub> (50.2 mg, 0.109 mmol) and DPES (76.6 mg, 0.220 mmol) was stirred for 1 h at room temperature. The solution was reduced to ca. 2 mL, and diethyl ether (35 mL) was added, forming a bright yellow air-stable precipitate. The powder was collected by filtration, washed with diethyl ether (2 × 10 mL), and dried under vacuum. Yield: 130 mg (73%). Yellow crystals were obtained by slow diffusion of diethyl ether into a dichloromethane solution of 1. <sup>1</sup>H NMR:  $\delta$  7.66–7.19 (m, 13H, Ar), 6.85 (dd, <sup>3</sup>J<sub>HH</sub> = 10.5, 7.8 Hz, 1H, Ar), 6.12 (s, 2H, Ar–CH<sub>2</sub>–), 5.25 (bs, 2H, NBD), 3.83 (bs, 2H, NBD), 3.15 (bs, 2H, NBD), 2.32 (q, <sup>3</sup>J<sub>HH</sub> = 7.5 Hz, 2H, –CH<sub>2</sub>–), 1.42 (bs, 2H, NBD), 1.16 (t, <sup>3</sup>J<sub>HH</sub> = 7.5 Hz, 3H, –CH<sub>3</sub>). Anal. Calcd for C<sub>29</sub>H<sub>29</sub>ClO<sub>2</sub>PrH: C, 60.2; H, 5.1; P, 5.4. Found: C, 60.3; H, 5.2; P, 5.4.

**Reaction of [ $\mu$ -IrCl(1,5-COD)]<sub>2</sub> with DPES. Formation of [IrCl(1,5-COD)(DPES)] (2).** Using a procedure similar to that for 1 with [ $\mu$ -IrCl(1,5-COD)]<sub>2</sub> (30.2 mg, 44.9  $\mu$ mol) and DPES (31.6 mg, 90.8  $\mu$ mol) gave complex 2 as an air-stable bright yellow powder. Yield: 50.3 mg (81%). <sup>1</sup>H NMR:  $\delta$  7.71–7.08 (m, 14H, Ar), 5.78 (s, 2H, Ar–CH<sub>2</sub>–), 5.16 (bs, 2H, COD), 3.00 (bs, 2H, COD), 2.34 (q, <sup>3</sup>J<sub>HH</sub> = 7.5 Hz, 2H, –CH<sub>2</sub>–), 2.26–1.28 (m, 8H, COD), 1.16 (t, <sup>3</sup>J<sub>HH</sub> = 7.5 Hz, 3H, –CH<sub>3</sub>). Anal. Calcd for C<sub>30</sub>H<sub>33</sub>ClO<sub>2</sub>PIr: C, 53.0; H, 4.8, P, 4.3. Found: C, 53.2; H, 5.2; P, 4.3.

**Reaction of [Rh(2,5-NBD)]<sub>2</sub>[CF<sub>3</sub>SO<sub>3</sub>] with DPES. Formation of [Rh(2,5-NBD)(DPES)][CF<sub>3</sub>SO<sub>3</sub>] (3).** [Rh(2,5-NBD)]<sub>2</sub>[CF<sub>3</sub>SO<sub>3</sub>] (53.2 mg, 0.122 mmol) and DPES (42.7 mg, 0.123 mmol) were dissolved in dichloromethane (10 mL). After the bright yellow solution was stirred for 30 min, the solvent was concentrated under vacuum to ca. 2 mL. Dropwise addition of *n*-hexane (20 mL) gave a yellow precipitate. Removal of the solvent and drying under vacuum gave the air-sensitive complex 3. Yield: 43.1 mg (51%). <sup>1</sup>H NMR (–40 °C in CD<sub>2</sub>-Cl<sub>2</sub>):  $\delta$  7.75–6.89 (m, 14H, Ar), 6.27 (bs, 2H, Ar–CH<sub>2</sub>–), 5.41 (bs, 2H, NBD), 3.92 (bs, 2H, NBD), 3.46 (bs, 2H, NBD), 2.14 (q, <sup>3</sup>J<sub>HH</sub> = 7.7 Hz, 2H, –CH<sub>2</sub>–) 1.43 (bs, 2H, NBD), 0.91 (t, <sup>3</sup>J<sub>HH</sub> = 7.7 Hz, 3H, –CH<sub>3</sub>). Anal. Calcd for C<sub>30</sub>H<sub>29</sub>F<sub>3</sub>O<sub>5</sub>PSRh: C, 52.1; H, 4.2; P, 4.5. Found: C, 52.9; H, 5.0; P, 4.3.

**Reaction of [Ir(1,5-COD)]<sub>2</sub>[BF<sub>4</sub>] with DPES. Formation of [IrH(1,5-COD)(DPES)][BF<sub>4</sub>] (4).** When [Ir(1,5-COD)]<sub>2</sub>[BF<sub>4</sub>] (91.3 mg, 0.184 mmol) and DPES (64.3 mg, 0.184 mmol) were mixed in dichloromethane (10 mL), the solution gradually changed color from dark red to light yellow within minutes. After 45 min an off-white powder was isolated by evaporation of the solvent and washed with diethyl ether (3 × 10 mL) and *n*-hexane (3 × 10 mL). Yield: 115 mg (83%). This air-stable product can be recrystallized by slow diffusion of diethyl ether into a solution of acetone. <sup>1</sup>H NMR:  $\delta$  7.79–7.03 (m, 14H, Ar), 6.87 (d, <sup>3</sup>J<sub>PH</sub> = 1.8 Hz, 1H, Ar–C(R)H–Ir), 5.86 (m, 1H, COD), 5.25 (m, 1H, COD), 4.68 (m, 2H, COD), 2.76–2.34 (m, 8H, COD), 2.24–1.86 (m, 2H, –CH<sub>2</sub>–), 0.68 (t, <sup>3</sup>J<sub>HH</sub> = 7.8 Hz, 3H, –CH<sub>3</sub>), –19.2 (d, <sup>2</sup>J<sub>PH</sub> = 13 Hz, 1H, Ir–H). <sup>13</sup>C{<sup>1</sup>H} NMR:  $\delta$  187.8 (s, –C(O)–), 154–126 (m, Ar), 99.9 (d, <sup>2</sup>J<sub>PC</sub> = 10 Hz, COD), 98.8 (d, <sup>2</sup>J<sub>PC</sub> = 14 Hz, COD), 95.1 (s, COD), 93.0 (s, COD), 92.3 (bs, Ar–C(R)H–Ir), 33.2 (bs, COD), 33.1 (bs, COD), 29.7 (d, <sup>3</sup>J<sub>PC</sub> = 3 Hz, COD), 28.5 (d, <sup>3</sup>J<sub>PC</sub> = 2 Hz, COD), 26.0 (s, –CH<sub>3</sub>), 8.83 (s, –CH<sub>2</sub>–) (assignment of <sup>1</sup>H and <sup>13</sup>C{<sup>1</sup>H} NMR signals were confirmed by <sup>1</sup>H{<sup>31</sup>P} and HMQC NMR experiments). Anal. Calcd for C<sub>30</sub>H<sub>33</sub>BF<sub>4</sub>O<sub>2</sub>PIr: C, 49.0; H, 4.5; P, 4.2. Found: C, 49.0; H, 4.7; P, 4.3.

**Reaction of [Rh(2,5-NBD)(PPh<sub>3</sub>)<sub>2</sub>][PF<sub>6</sub>] with DPES. Formation of [RhH(PPh<sub>3</sub>)<sub>2</sub>(DPES)][PF<sub>6</sub>] (5).** A cooled (–60 °C) dihydrogen saturated solution of dichloromethane (10 mL) was transferred by stainless steel cannula to a Schlenk tube containing [Rh(2,5-NBD)(PPh<sub>3</sub>)<sub>2</sub>][PF<sub>6</sub>] (107 mg, 0.124 mmol) and DPES (43.1 mg, 0.124 mmol). The solution was allowed

(26) Giordano, G.; Crabtree, R. H. *Inorg. Synth.* **1990**, *28*, 88.

(27) Herde, J. L.; Lambert, J. C.; Senoff, C. V. *Inorg. Synth.* **1974**, *15*, 19.

(28) Schenck, T. G.; Downes, J. M.; Milne, C. R. C.; Mackenzie, P. B.; Boucher, H.; Whelan, J.; Bosnich, B. *Inorg. Chem.* **1985**, *24*, 2334.

(29) van der Ent, A.; Onderdelinden, A. L. *Inorg. Synth.* **1973**, *14*, 92.

(30) Schrock, R. R.; Osborn, J. A. *J. Am. Chem. Soc.* **1976**, *98*, 2143.

to reach room temperature, and the light brown solution was stirred for 30 min. An argon atmosphere was introduced, and after a further 30 min the solution had become dark brown. The solvent was removed under vacuum, resulting in a brown, air-stable powder, which was washed with diethyl ether (3 × 10 mL) and *n*-hexane (2 × 10 mL). Yield: 112 mg (81%). <sup>1</sup>H NMR (CD<sub>2</sub>Cl<sub>2</sub>): δ 7.62–6.92 (m, 13H, Ar), 6.17 (m, 1H, Ar), 6.09 (bd, <sup>2</sup>J<sub>RhH</sub> = 20 Hz, 1H, Ar–CH(R)–Rh), 1.27 (m, 2H, –CH<sub>2</sub>–), 0.56 (t, <sup>3</sup>J<sub>HH</sub> = 7.2 Hz, 3H, –CH<sub>3</sub>), –17.3 (ddt, <sup>1</sup>J<sub>RhH</sub> = 20 Hz, <sup>2</sup>J<sub>PH</sub> = 16, 10 Hz, 1H, Rh–H). <sup>13</sup>C{<sup>1</sup>H} NMR (CD<sub>2</sub>Cl<sub>2</sub>): δ 184.5 (s, –C(O)–), 151–126 (md, Ar), 103.8 (dddd, <sup>1</sup>J<sub>RhC</sub> = 87 Hz, <sup>2</sup>J<sub>PC</sub> = 23, 10, 3 Hz, Ar–CH(R)–Rh), 26.1 (s, –CH<sub>3</sub>), 8.29 (s, –CH<sub>2</sub>–) (assignment of <sup>1</sup>H and <sup>13</sup>C{<sup>1</sup>H} NMR signals were confirmed by <sup>1</sup>H{<sup>31</sup>P} and HMQC NMR experiments). Anal. Calcd for C<sub>58</sub>H<sub>51</sub>F<sub>6</sub>O<sub>2</sub>P<sub>4</sub>Rh: C, 62.1; H, 4.6; P, 11.0. Found: C, 61.8; H, 4.8; P, 11.0.

**Reaction of [Rh(2,5-NBD)<sub>2</sub>][CF<sub>3</sub>SO<sub>3</sub>] with DPBE. Formation of [Rh(2,5-NBD)(DPBE)][CF<sub>3</sub>SO<sub>3</sub>] (6).** Using a procedure similar to that for **3** with [Rh(2,5-NBD)<sub>2</sub>][CF<sub>3</sub>SO<sub>3</sub>] (49.7 mg, 0.114 mmol) and DPBE (34.9 mg, 0.114 mmol) gave complex **6** as an air-sensitive yellow powder. Yield: 56 mg (75%). <sup>1</sup>H NMR: δ 7.51–7.02 (m, 14H, Ar), 4.72 (s, 2H, –CH<sub>2</sub>–), 4.43 (bs, 2H, NBD), 3.96 (bs, 2H, NBD), 3.54 (s, 3H, –CH<sub>3</sub>), 1.43 (bs, 2H, NBD). Anal. Calcd for C<sub>28</sub>H<sub>27</sub>F<sub>3</sub>O<sub>4</sub>PSRh: C, 51.9; H, 4.4; P, 4.7. Found: C, 52.2; H, 4.6; P, 4.6.

**Reaction of [Ir(1,5-COD)<sub>2</sub>][BF<sub>4</sub>] with DPBE. Formation of [Ir(1,5-COD)(DPBE)][BF<sub>4</sub>] (7).** Using a procedure similar to that for **3** with [Ir(1,5-COD)<sub>2</sub>][BF<sub>4</sub>] (95.2 mg, 0.192 mmol) and DPBE (59.2 mg, 0.193 mmol) gave complex **7** as a light orange powder. The complex was too unstable for microanalysis. Yield: 107 mg (81%). <sup>1</sup>H NMR (CD<sub>2</sub>Cl<sub>2</sub>): δ 7.87–7.35 (m, 14H, Ar), 5.24 (bs, 2H, COD), 5.09 (s, 2H, –CH<sub>2</sub>–), 3.77 (s, 3H, –CH<sub>3</sub>), 3.18 (bs, 2H, COD), 2.57–1.63 (m, 8H, COD).

**Reaction of [Rh(2,5-NBD)<sub>2</sub>][CF<sub>3</sub>SO<sub>3</sub>] with DPBE. Formation of [Rh(DPBE)<sub>2</sub>][CF<sub>3</sub>SO<sub>3</sub>] (8).** A solution of [Rh(2,5-NBD)<sub>2</sub>][CF<sub>3</sub>SO<sub>3</sub>] (65.7 mg, 0.151 mmol) and DPBE (93.4 mg, 0.305 mmol) in dichloromethane (10 mL) was stirred for 10 min. A freeze–pump–thaw cycle replaced the argon atmosphere by molecular hydrogen. When it was stirred for 15 min, the solution gradually changed color from red to yellow. The atmosphere of molecular hydrogen was replaced by argon, and after 45 min the solution was once again red. Reduction of the solvent volume to ca. 1 mL followed by addition of diethyl ether (20 mL) resulted in a bright orange air-sensitive precipitate. The powder was washed with diethyl ether (3 × 5 mL) and dried under vacuum. Yield: 103 mg (85%). <sup>1</sup>H NMR: δ 7.63–6.78 (m, 28H, Ar), 4.58 (s, 4H, –CH<sub>2</sub>–), 3.78 (s, 6H, –CH<sub>3</sub>). Anal. Calcd for C<sub>41</sub>H<sub>38</sub>F<sub>3</sub>O<sub>5</sub>P<sub>2</sub>SRh: C, 56.9; H, 4.4; P, 7.2. Found: C, 55.2; H, 4.8; P, 7.1.

**Reaction of [μ-IrCl(C<sub>8</sub>H<sub>14</sub>)<sub>2</sub>]<sub>2</sub> with DPBE. Formation of [IrHCl(DPBE)<sub>2</sub>] (9a,b).** THF (5 mL) was transferred to a Schlenk tube containing [μ-IrCl(C<sub>8</sub>H<sub>14</sub>)<sub>2</sub>]<sub>2</sub> (54.4 mg, 60.7 μmol), resulting in an orange suspension. A solution of DPBE (74.4 mg, 0.243 mmol) in THF (5 mL) was transferred to the stirred suspension, which instantly became clear. After a couple of minutes the solution became light yellow and was stirred for a further 30 min. Filtration removed traces of metallic iridium, and the solution was reduced to ca. 2 mL. Addition of *n*-hexane (20 mL) formed an off-white precipitate. The powder was isolated, washed with additional *n*-hexane (2 × 15 mL), and dried under vacuum. Yield: 88.8 mg (87%). <sup>1</sup>H NMR (C<sub>6</sub>D<sub>6</sub>): δ 8.37–6.49 (m, 56H, Ar), 7.54 (d, <sup>3</sup>J<sub>PH</sub> = 5.0 Hz, 1H, Ar–CH(R)–Ir, **9b**), 6.79 (d, <sup>3</sup>J<sub>PH</sub> = 7.4 Hz, 1H, Ar–CH(R)–Ir, **9a**), 5.41 (d, <sup>2</sup>J<sub>HH</sub> = 13 Hz, 1H, –CH<sub>2</sub>–, **9b**), 5.01 (d, <sup>2</sup>J<sub>HH</sub> = 12 Hz, 1H, –CH<sub>2</sub>–, **9a**), 4.29 (d, <sup>2</sup>J<sub>HH</sub> = 13 Hz, 1H, –CH<sub>2</sub>–, **9b**), 4.04 (d, <sup>2</sup>J<sub>HH</sub> = 13 Hz, 1H, –CH<sub>2</sub>–, **9a**), 3.70 (s, 3H, –CH<sub>3</sub>, **9b**), 3.29 (s, 3H, –CH<sub>3</sub>, **9b**), 2.85 (s, 3H, –CH<sub>3</sub>, **9a**), 2.58 (s, 3H, –CH<sub>3</sub>, **9a**), –19.8 (dd, <sup>2</sup>J<sub>PH</sub> = 21, 11 Hz, 1H, Ir–H, **9a**), –20.0 (t, <sup>2</sup>J<sub>PH</sub> = 16 Hz, 1H, Ir–H, **9b**). <sup>13</sup>C{<sup>1</sup>H} NMR (C<sub>6</sub>D<sub>6</sub>): δ 135–126 (md, Ar), 91.4 (d, <sup>2</sup>J<sub>PC</sub> = 98 Hz, Ar–CH(R)–Ir), 79.8 (d,

**Table 5. Crystallographic Data for Complexes 1 and 4**

formula	C <sub>29</sub> H <sub>29</sub> ClO <sub>2</sub> PRh (1)	C <sub>30</sub> H <sub>33</sub> BF <sub>4</sub> O <sub>2</sub> PIr (4)
fw	578.85	735.54
cryst size, mm <sup>3</sup>	0.25 × 0.17 × 0.07	0.24 × 0.23 × 0.06
cryst syst	triclinic	orthorhombic
space group	P1̄ (No. 2)	Pna2 <sub>1</sub> (No. 33)
a, Å	9.415(2)	19.433(4)
b, Å	9.886(2)	14.654(3)
c, Å	16.318(3)	9.944(2)
α, deg	93.90(3)	90
β, deg	100.95(3)	90
γ, deg	117.50(3)	90
V, Å <sup>3</sup>	1301.3(5)	2831.7(10)
Z	2	4
d <sub>calcd</sub> , g cm <sup>-3</sup>	1.477	1.725
diffractometer	smart CCD system	smart CCD system
radiation (graphite monochr)	Mo Kα (0.710 73 Å)	Mo Kα (0.710 73 Å)
temp, K	293(2)	293(2)
μ, mm <sup>-1</sup>	0.845	4.824
scan method	ω	ω
2θ(max), deg	60	60
abs cor	ω-scan/multiscan	ω-scan/multiscan
T <sub>min</sub>	0.729	0.621
T <sub>max</sub>	1.000	1.000
R <sub>int</sub>	0.0249	0.0430
h	–13 to +12	–24 to +28
k	–11 to +14	–16 to +20
l	–20 to +23	–11 to +13
total no. of rflns	11 064	23 072
no. of unique rflns	7691	8125
no. of obsd rflns (2σ(I))	6090	6129
no. of params refined	308	357
R	0.0370	0.0287
R <sub>w</sub>	0.0543	0.0583
rfln:param ratio	24.97	22.76
resid electron density, e Å <sup>-3</sup>	0.504	0.725

<sup>3</sup>J<sub>PC</sub> = 9 Hz, –CH<sub>2</sub>–), 79.2 (d, <sup>3</sup>J<sub>PC</sub> = 11 Hz, –CH<sub>2</sub>–), 63.6 (s, –CH<sub>3</sub>), 61.2 (s, –CH<sub>3</sub>), 58.6 (bs, Ar–CH(R)–Ir), 54.6 (s, –CH<sub>3</sub>), 52.5 (s, –CH<sub>3</sub>) (assignments of <sup>1</sup>H and <sup>13</sup>C{<sup>1</sup>H} NMR signals were confirmed by <sup>1</sup>H{<sup>31</sup>P} and HMQC NMR experiments). Anal. Calcd for C<sub>40</sub>H<sub>38</sub>ClO<sub>2</sub>P<sub>2</sub>Ir: C, 57.1; H, 4.6; P, 7.3. Found: C, 56.8; H, 4.7; P, 6.9.

**X-ray Structural Analyses of Complexes 1 and 4.** Single crystals were grown from dichloromethane/diethyl ether (**1**) and acetone/diethyl ether (**4**) solutions at 25 °C under an atmosphere of argon. The crystal data and data collection and refinement details are provided in Table 5. Intensity data were collected at 293 K with a Smart CCD system using ω scans and a rotating anode with Mo Kα radiation (λ = 0.710 69 Å). All reflections were corrected for Lorentz and polarization effects as well as absorption.<sup>31</sup> No significant changes in intensities were noticed throughout the data collections.

The structures were solved by Patterson methods using SHELXS-86,<sup>32</sup> while the structure refinements were performed on F<sup>2</sup> using SHELXL-93.<sup>33</sup> All non-H atoms were refined with anisotropic displacement parameters, while the hydrogen atoms were constrained to the parent site, using a riding model. The absolute structure of the noncentrosymmetric complex **4** was determined using the Flack parameter 0.005–(6).<sup>34</sup> The coordinated hydride in **4** was located from the difference Fourier map after anisotropic refinement, and then

(31) Sheldrick; G. M. SADABS: Program for Absorption Correction; University of Göttingen, Göttingen, Germany, 1996.

(32) Sheldrick; G. M. SHELXL-86: Structure Solution Program; University of Göttingen, Göttingen, Germany, 1990.

(33) Sheldrick; G. M. SHELXL-93: Structure Refinement Program; University of Göttingen, Göttingen, Germany, 1993.

(34) Flack, H. D. *Acta Crystallogr.* **1983**, *A39*, 876.

the hydride was isotropically refined. No high electron density residues were found in the structures.

**Acknowledgment.** Financial support by the TFR (The Swedish Research Council for Technological Sciences) and the NFR (The Swedish Natural Science Research Council) is gratefully acknowledged.

**Supporting Information Available:** Tables of crystal data and structure refinement, atomic coordinates, bond lengths and angles, anisotropic displacement parameters, and hydrogen coordinates for complexes **1** and **4** and a table of least-squares planes for **1**. This material is available free of charge via the Internet at <http://pubs.acs.org>.

OM980929G